

Sussex Research

A genetically encoded reporter of synaptic activity in vivo

Elena Dreosti, Benjamin Odermatt, Mario M Dorostkar, Leon Lagnado

Publication date

01-01-2009

Licence

This work is made available under the **Copyright not evaluated** licence and should only be used in accordance with that licence. For more information on the specific terms, consult the repository record for this item.

Citation for this work (American Psychological Association 7th edition)

Dreosti, E., Odermatt, B., Dorostkar, M. M., & Lagnado, L. (2009). *A genetically encoded reporter of synaptic activity in vivo* (Version 1). University of Sussex. <https://hdl.handle.net/10779/uos.23398781.v1>

Published in

Nature Methods

Link to external publisher version

<https://doi.org/10.1038/nmeth.1399>

Copyright and reuse:

This work was downloaded from Sussex Research Open (SRO). This document is made available in line with publisher policy and may differ from the published version. Please cite the published version where possible. Copyright and all moral rights to the version of the paper presented here belong to the individual author(s) and/or other copyright owners unless otherwise stated. For more information on this work, SRO or to report an issue, you can contact the repository administrators at sro@sussex.ac.uk. Discover more of the University's research at <https://sussex.figshare.com/>

A genetically encoded reporter of synaptic activity in vivo

Article (Unspecified)

Dreosti, Elena, Odermatt, Benjamin, Dorostkar, Mario M and Lagnado, Leon (2009) A genetically encoded reporter of synaptic activity in vivo. *Nature Methods*, 6. pp. 883-889. ISSN 1548-7091

This version is available from Sussex Research Online: <http://sro.sussex.ac.uk/id/eprint/46585/>

This document is made available in accordance with publisher policies and may differ from the published version or from the version of record. If you wish to cite this item you are advised to consult the publisher's version. Please see the URL above for details on accessing the published version.

Copyright and reuse:

Sussex Research Online is a digital repository of the research output of the University.

Copyright and all moral rights to the version of the paper presented here belong to the individual author(s) and/or other copyright owners. To the extent reasonable and practicable, the material made available in SRO has been checked for eligibility before being made available.

Copies of full text items generally can be reproduced, displayed or performed and given to third parties in any format or medium for personal research or study, educational, or not-for-profit purposes without prior permission or charge, provided that the authors, title and full bibliographic details are credited, a hyperlink and/or URL is given for the original metadata page and the content is not changed in any way.

A genetically encoded reporter of synaptic activity *in vivo*

Elena Dreosti, Benjamin Odermatt, Mario M Dorostkar & Leon Lagnado

To image synaptic activity within neural circuits, we tethered the genetically encoded calcium indicator (GECI) GCaMP2 to synaptic vesicles by fusion to synaptophysin. The resulting reporter, SyGCaMP2, detected the electrical activity of neurons with two advantages over existing cytoplasmic GECIs: it identified the locations of synapses and had a linear response over a wider range of spike frequencies. Simulations and experimental measurements indicated that linearity arises because SyGCaMP2 samples the brief calcium transient passing through the presynaptic compartment close to voltage-sensitive calcium channels rather than changes in bulk calcium concentration. *In vivo* imaging in zebrafish demonstrated that SyGCaMP2 can assess electrical activity in conventional synapses of spiking neurons in the optic tectum and graded voltage signals transmitted by ribbon synapses of retinal bipolar cells. Localizing a GECI to synaptic terminals provides a strategy for monitoring activity across large groups of neurons at the level of individual synapses.

Understanding the function of neural circuits requires the monitoring of electrical signals generated by groups of neurons as well as the transmission of signals at the synaptic junctions that connect them. Measuring where, when and how strongly synapses are active in a circuit is therefore an important technical challenge.

Electrophysiological methods record electrical activity with unparalleled resolution but are difficult to apply *in vivo* or to more than one neuron at a time. Optical techniques show promise for monitoring electrical activity across many neurons, especially using fluorescent calcium indicators that report the opening of calcium channels when a neuron is excited^{1,2}. Synthetic calcium dyes are available with a range of properties, but genetically encoded calcium indicators (GECIs) offer the important advantage of targeting to known classes of neurons^{3–5}. Detecting the activation of synapses has proven more difficult. The best general approach thus far has been the reporter protein synaptopHluorin, which signals the loss of protons from a synaptic vesicle upon fusion⁶. But the sensitivity of synaptopHluorin is limited by background fluorescence generated by expression on the cell surface. In intact circuits, synaptopHluorin has only provided useful signals after prolonged stimulation and spatial averaging^{4,7,8}. The analysis of circuit function would be aided greatly by a genetically encoded

reporter that detects the activation of individual synapses by single action potentials (APs).

Here we report a new approach for detecting synaptic activity optically: the localization of a GECI to the presynaptic terminal to sense calcium influx triggering neurotransmitter release⁹. The presynaptic terminal is a small compartment containing a high density of voltage-sensitive calcium channels and usually experiences the largest calcium transient in response to a spike¹⁰. The reporter we designed, SyGCaMP2, is a fusion of GCaMP2 (ref. 11) to the cytoplasmic side of synaptophysin, a transmembrane protein in synaptic vesicles.

Using cultured hippocampal neurons and simulations, we demonstrated that SyGCaMP2 has the potential to detect single spikes at individual synapses as well as activity occurring in short bursts. By imaging zebrafish *in vivo*, we demonstrated that SyGCaMP2 can be used to monitor visual activity in conventional synapses of spiking neurons in the optic tectum and ribbon synapses of graded neurons in the retina, sampling hundreds of terminals simultaneously.

RESULTS

Rationale for localizing GCaMP2 to presynaptic compartments

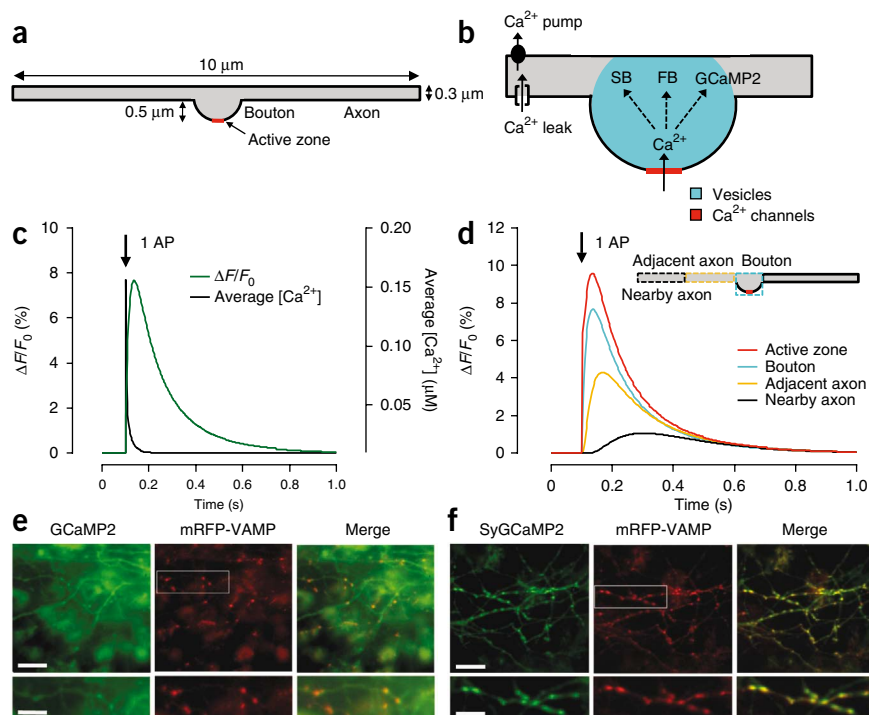
To investigate how a GECI responds to synaptic calcium signals, we constructed a Virtual Cell simulation environment model of calcium dynamics in the synaptic bouton and neighboring axon of a hippocampal neuron, designed to reproduce optical measurements made using the fluorescent Ca^{2+} indicator fura-2¹² (Fig. 1a,b, Supplementary Fig. 1, Supplementary Table 1 and Supplementary Note). We then incorporated a GECI into the model. We chose GCaMP2 because it displays a large fluorescence increase on binding calcium (approximately sixfold) and seems promising for detecting electrical activity⁵. Using GCaMP2 free in the cytoplasm, one would expect the peak response to a single AP recorded within a bouton to be ~8% (Fig. 1c), which is within the limits of detectability in many imaging situations. The model also predicts that although the spatially averaged Ca^{2+} signal in the bouton recovers with a half-life ($t_{1/2}$) of 2 ms, the SyGCaMP2 signal recovers with $t_{1/2}$ of 360 ms (Fig. 1c), which is similar to the rate at which the reporter relaxes back to a state of reduced fluorescence after Ca^{2+} ions dissociate¹¹. These simulations underline a key property of the currently available GECIs:

Medical Research Council Laboratory of Molecular Biology, Cambridge, UK. Correspondence should be addressed to L.L. (ll1@mrc-lmb.cam.ac.uk).

RECEIVED 6 APRIL; ACCEPTED 7 OCTOBER; PUBLISHED ONLINE 8 NOVEMBER 2009; DOI:10.1038/NMETH.1399

Figure 1 | Modeling GCaMP2 responses in the synapse and axon. (a) Geometry of the two-dimensional model implemented in the Virtual Cell simulation environment. (b) Calcium buffers, channels and pumps used in the model. Distribution of calcium channels at the active zone is shown in red, and distribution of synaptic vesicles is in cyan. FB, fast, mobile buffer; SB, slow, immobile buffer. (c) Modeled response of GCaMP2 (1 μM) to a single spike ($\Delta F/F_0$) calculated as the relative change in GCaMP2 fluorescence in a region of interest over the bouton. The spatially averaged Ca^{2+} concentration, reported by cytoplasmic fura-2, was also averaged over the whole bouton. This signal was obtained by adjusting the parameters of the model to reproduce the response to a single spike reported by fura-2¹². Note the slower GCaMP2 signal as compared with the Ca^{2+} transient.

(d) Simulations of GCaMP2 signals at different distances from calcium channels: within 50 nm of the active zone, averaged over the bouton, over a 2.25- μm length of an axon adjacent to the bouton and over the next 2.25- μm length of a nearby axon. (e,f) Fluorescence images of neuronal-glial cultures of rat hippocampi expressing cytoplasmic GCaMP2 (e) or synaptic SyGCaMP2 (f). Expression of the synaptic marker mRFP-VAMP is also shown. The rectangular field of view is expanded in the images below. Only SyGCaMP2 visualizes all synaptic boutons marked by mRFP-VAMP. For equipment and settings, see **Supplementary Methods**. Scale bars, 20 μm (top) and 10 μm (bottom).



they are not in rapid equilibrium with brief Ca^{2+} transients generated close to voltage-sensitive calcium channels.

Might it be possible to improve the GCaMP2 signal generated by a spike by sampling it closer to calcium channels by, for instance, fusion of GCaMP2 to the channels themselves? An immediate disadvantage of this strategy will be the small number of GCaMP2 molecules that might sense the calcium transient, which will limit the signal-to-noise ratio (SNR). Simulations also predicted that placing GCaMP2 within 50 nm of the active zone will generate signals that differ little from averages obtained over the whole bouton, even in the absence of noise (**Fig. 1d**). In contrast, GCaMP2 signals in the axon will be slow and small, and so it is essential to prevent them from contaminating fluorescence collected from the synaptic bouton. These simulations therefore suggest that the best combination of SNR and temporal resolution will be obtained by distributing GCaMP2 molecules throughout the presynaptic compartment, so we investigated this strategy experimentally.

To localize GCaMP2 to synaptic terminals, we fused it to the cytoplasmic side of the vesicular protein synaptophysin to make SyGCaMP2. We chose synaptophysin because it is localized to synaptic vesicles with relatively little expression on the surface membrane¹³. SyGCaMP2 marked synaptic boutons in cultured hippocampal neurons as clearly as the synaptic marker mRFP-VAMP (**Fig. 1e,f**) and also responded to calcium influx. We imaged a region of synapses containing SyGCaMP2 (**Fig. 2a**), and we collected images to measure the change in fluorescence during a train of 10 APs delivered at 20 Hz (**Supplementary Video 1**). In this example, 10 APs caused a relative fluorescence increase of ~75% (**Fig. 2b**). Notably, tethering GCaMP2 to synaptophysin did not hinder vesicle fusion measured using the fluorescent dye FM4-64

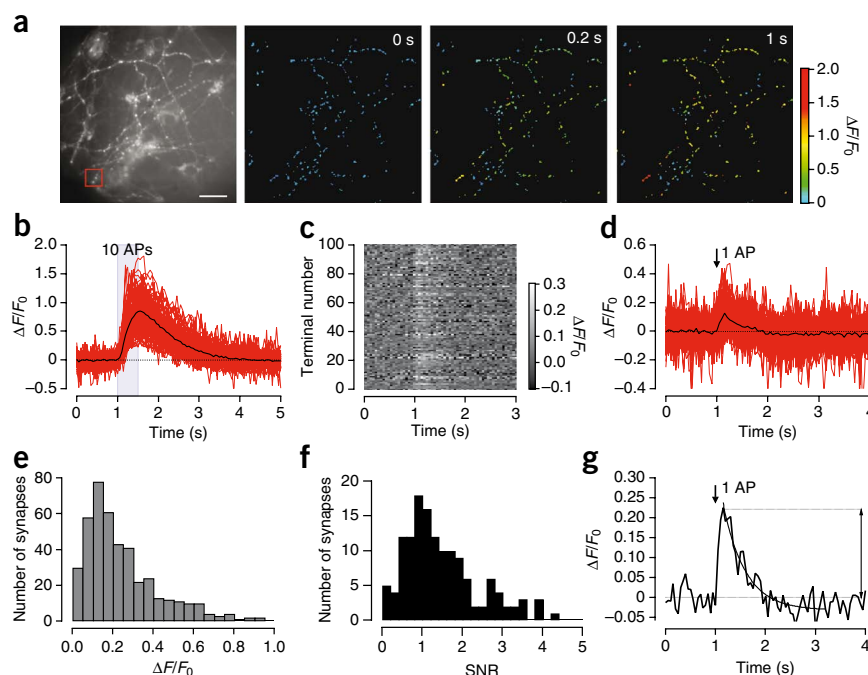
(**Supplementary Fig. 2**). SyGCaMP2 therefore has two important advantages over GECI mobile in the cytoplasm: the immediate identification of synaptic boutons at rest, and the detection of calcium influx at sites close to voltage-sensitive calcium channels.

Sensitivity and dynamic range of SyGCaMP2

Several GECIs have been tested as detectors of spike activity^{3–5}. Among the most sensitive is D3cpv, which generates a signal of ~8% in response to a single AP when the signal is collected from the soma. A limitation of D3cpv, as well as synthetic calcium indicators of high affinity, is saturation of the response after just 2–3 APs. This limitation reflects the high affinity of the reporter and the slow decay of the calcium transient in a volume as large as the soma (~4 s)¹⁴. GCaMP2 also has a high affinity for calcium ($K_d \sim 150$ nM), but we found that its localization to the synaptic bouton, where the calcium transient is very brief, extended the range of firing rates that could be reported.

We examined the responses of SyGCaMP2 to single APs (**Fig. 2c,d**). The normalized response ($\Delta F/F_0$) was $11.50 \pm 0.01\%$ and decayed with the off-rate of the reporter ($t_{1/2} = 210$ ms; **Fig. 2d**). Notably, the amplitude of signals varied widely between different boutons, from ~4% to ~90% (**Fig. 2e**). Such variations in the amplitude of the presynaptic calcium transient are likely to contribute to the heterogeneous-release probability of synapses in these cultures^{15,16}. As a consequence, the SNR for detection of a spike depended on the bouton at which it was measured. About 20% of boutons in the region shown in **Figure 2a** had an SNR >2 for a single spike (**Fig. 2f**), which is similar to the performance achieved with the synthetic indicator Fluo-4F in dendrites¹⁷. A simple way to improve the SNR was to average the response over several boutons on

Figure 2 | Presynaptic calcium signals visualized with SyGCaMP2. (a) Fluorescence image of cultured neurons expressing SyGCaMP2 (left) and pseudocolored images showing the relative change in fluorescence at rest, then 0.2 s and 1 s after the beginning of a train of 10 APs delivered at 20 Hz. Note the variability in the amplitude of the presynaptic calcium signal between different boutons. For equipment and settings, see **Supplementary Methods**. Scale bar, 20 μm . (b) SyGCaMP2 responses from 20 individual boutons shown in **a** (red traces) and their average (black). (c) Fluorescence responses to one AP from 100 synapses in the field in **a**. (d) SyGCaMP2 responses to a single AP from 20 individual boutons (red traces) and the average (black), for the field shown in **a**. (e) Histogram showing the distribution of SyGCaMP2 responses to one AP measured at their peak. The mean amplitude was 11.5%. (f) The distribution of SNRs measured at different boutons in response to one AP, from the field shown in **a**. SNR was measured as the peak amplitude of the response divided by the s.d. in the signal at rest, as shown in **g**. (g) Response to a single AP averaged from three neighboring boutons shown in the red box in **a**. Note that this was a single trial. The peak amplitude of the signal was 22%, and the noise in the baseline had an s.d. of 3%, yielding an SNR of 7.3 for the average.



a short stretch of axon. For instance, we analyzed the signal from the three boutons in the image in **Figure 2a**, when the SNR was 7.3 for a single AP (**Fig. 2g**). SyGCaMP2 therefore allowed the detection of individual spikes with a good degree of reliability and revealed heterogeneity in the calcium signal triggering vesicle release at different terminals.

To investigate the range of activities that SyGCaMP2 might report, we delivered trains of APs of various durations at a fixed frequency of 20 Hz (**Fig. 3a**). The peak amplitude of the response was linear up to about 5–8 APs, depending on the culture in which it was measured, and a plateau was not reached until 10–20 APs (**Fig. 3b**). The response of SyGCaMP2 in hippocampal boutons was therefore linear over a range sufficient to detect short bursts of APs. This property originated from its localization to the presynaptic bouton, not from its attachment to synaptophysin, because

GCaMP2 signals at the synapse were similar (**Fig. 3b**). When we delivered two trains of 10 APs 6 s apart, the responses were almost identical, indicating that these stimuli did not generate substantial spatial rearrangements of the reporter (**Supplementary Fig. 2**).

SyGCaMP2 generated a maximum response of $\sim 70\%$ at a frequency of 20 Hz, in agreement with the model (**Fig. 3c**). To determine whether the plateau was caused by saturation of the reporter, we imposed changes in internal calcium concentration by permeabilizing the surface membrane using ionomycin (**Fig. 3d**). In the presence of 0 Ca^{2+} and 10 mM EGTA, the fluorescence reached a minimum and then increased 5.2-fold on addition of 2.5 mM Ca^{2+} , 0 EGTA. The relative increase in fluorescence of SyGCaMP2 going from the calcium-free to fully calcium-bound state was therefore very close to the value of 4–5-fold measured for GCaMP2 *in vitro*¹¹. In contrast, the steady response of SyGCaMP2

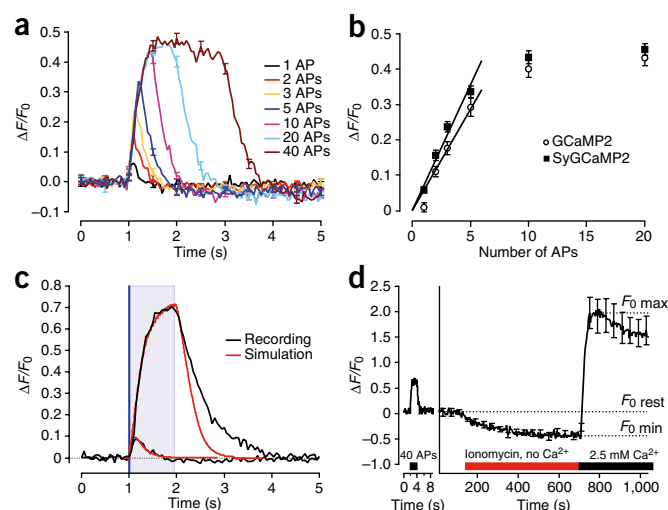
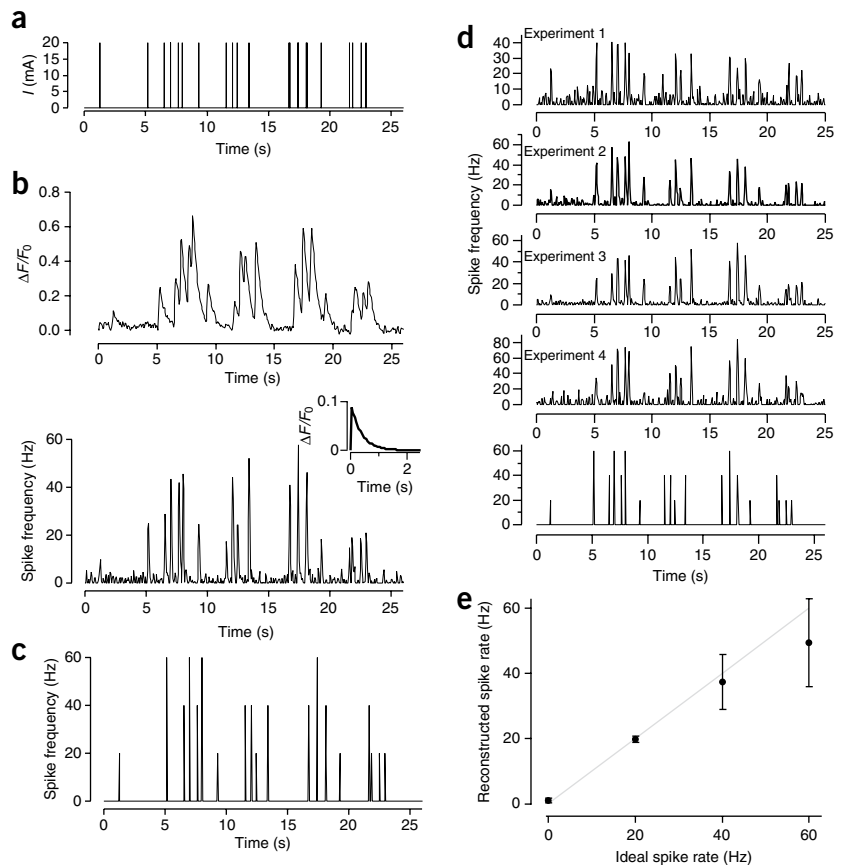


Figure 3 | The dynamic range of SyGCaMP2 responses. (a) Average SyGCaMP2 responses to trains of 1, 2, 3, 5, 10, 20 and 40 APs at 20 Hz. Each trace represents 500 synapses from six different coverslips. Error bars, s.e.m. (b) Peak amplitude of the SyGCaMP2 response taken from **a** as a function of the number of APs delivered. GCaMP2 responses are also plotted (error bars, s.e.m.; $n = 450$ synapses from five different coverslips). When using GCaMP2, boutons were identified by coexpressing mRFP-VAMP2. The response of SyGCaMP2 was linear up to ~ 8 APs, with a proportionality constant of $7 \pm 0.3\%$ per AP for SyGCaMP2 and $5 \pm 0.4\%$ for GCaMP2. (c) Comparison of experimental SyGCaMP2 measurements (recording) and their simulations. The model accurately predicts the response to one AP as well as the saturating response to 20 APs at 20 Hz. The model does not account for the slower recovery of the SyGCaMP2 signal after the introduction of larger calcium loads. (d) SyGCaMP2 response to 40 APs delivered at 20 Hz (70% increase). Neurons were then perfused with ionomycin (5 μM), 0 Ca^{2+} and 10 mM EGTA. The minimum fluorescence ($\Delta F/F_{0 \text{ min}}$) was -0.55 relative to rest. The external $[\text{Ca}^{2+}]$ was then increased to 2.5 mM to saturate SyGCaMP2. The peak signal ($\Delta F/F_{0 \text{ max}}$) was 2.1. Assuming a Hill coefficient of 4 for the binding of Ca^{2+} to GCaMP2 and a K_d of 150 nM, the resting free $[\text{Ca}^{2+}]$ was estimated to be ~ 2 nM.

Figure 4 | Deconvolution of SyGCaMP2 signals to monitor spike activity. (a) A 'physiological' stimulus pattern (1 ms; current (I) = 20 mA) delivered to the hippocampal cultures simulating the spike activity recorded in the hippocampus of a sleeping rat *in vivo* (data courtesy of M. Jones, University of Bristol). (b) SyGCaMP2 signal averaged from ten synaptic boutons of a single neuron responding to the stimulus in a (top). Images were acquired in 50-ms intervals. Spike frequency reconstructed by deconvolution of the SyGCaMP2 signal with the impulse response shown in the inset (decaying with τ = 250 ms; bottom). (c) The ideal reconstruction of spike frequency obtained by counting spikes into 50-ms time bins (the frame duration when imaging SyGCaMP2). Note that the reconstruction agrees closely with the ideal for brief bursts of spikes measured physiologically. (d) Spike frequency reconstructed by deconvolution for four different SyGCaMP2 experiments (each from a different coverslip). SyGCaMP2 signals were averaged from ten synaptic boutons each. The bottom graph shows the ideal reconstruction from c for comparison. (e) The reconstructed spike rate against the ideal spike rate for experiments shown in d (error bars, s.e.m.).



to a train at 20 Hz was only 30% of this maximum (Fig. 3d), and the model accounted for this by the balance between the average rate of Ca^{2+} influx and diffusion of Ca^{2+} out of the bouton into the axon (Fig. 3c). The avoidance of saturation at 20 Hz allowed the maximum response of SyGCaMP2 to increase at higher spike frequencies: the initial rate of rise of the SyGCaMP2 signal was proportional to frequencies up to ~80 Hz (Supplementary Fig. 1).

Localizing SyGCaMP2 to synaptic terminals

One approach by which the activity of neurons can be assessed from calcium signals was deconvolution using a kernel derived from the response to a single spike^{18,19}. Deconvolution is only useful while the response of the reporter is linear and has therefore been difficult to use with cytoplasmic GECIs. The wider linear range of SyGCaMP2 prompted us to investigate whether deconvolution might be a useful approach with this reporter (Fig. 4a–c). By blocking intrinsic network activity and applying a 'physiological' spiking pattern (Fig. 4a), we mimicked hippocampal activity in a sleeping rat. SyGCaMP2 signals were averaged over ten synapses along one process (Fig. 4b) and deconvolved using an impulse response measured in response to single APs to yield a spike frequency trace. We imaged at 20 Hz, so the ideal reconstruction (Fig. 4c) counted spikes in 50-ms time bins. There were several points of agreement between the experimental and idealized reconstructions: we detected single APs and observed variations in the number of APs per burst. We compared the reconstruction from four different cultures (Fig. 4d), and summarized the quality of reconstruction with a plot of the reconstructed against the ideal spike rate (Fig. 4e). These results indicate that localizing a GECI to the synaptic bouton extended the utility of deconvolution to bursts of spikes lasting seconds at frequencies up to ~10 Hz.

Using SyGCaMP2 to monitor synaptic activity *in vivo*

To investigate the utility of SyGCaMP2 *in vivo*, we transiently expressed the reporter in the optic tectum of zebrafish using the α -tubulin promoter^{20,21}. The tectum receives visual information from retinal ganglion cells as well as integrating inputs from other sensory systems²². We imaged a single optical section through the tectum in a larval fish at 9 d after fertilization and identified a region in which 100 synaptic terminals labeled with SyGCaMP2 could be distinguished (Fig. 5a–c). Tectal neurons demonstrated very little spontaneous activity²³, but a subset of 12 synaptic boutons could be activated by an electric field (Fig. 5d) or by light (Fig. 5e). These synapses (Fig. 5c) appeared to follow the trajectory of a single axonal process. The 'minimal response' to a single 1-ms pulse of the electric field was easily detectable, with an average amplitude of $\Delta F/F_0$ = 100% and decaying with a time constant (τ) = 350 ms. In comparison, a train of 20 pulses at 20 Hz generated a response of $\Delta F/F_0$ = 400% (data not shown). Thus, although we could not know how many spikes this 'minimal response' reflected, it was far from saturation and provided a kernel by which we could use deconvolution to estimate relative spike rates.

To allow comparison with results obtained in cultured neurons, we stimulated the fish with the same pulse pattern as in Figure 4a. We averaged the resulting SyGCaMP2 signal from one trial over the 12 responding synapses and deconvolved this trace using the 'minimal response' as a kernel to provide the relative spike frequency (RSF) (Fig. 5f). We imaged at 10 Hz (Supplementary Video 2), so the ideal reconstruction (Fig. 5f) counted spikes in 100-ms time bins. There were several points of agreement between the experimental and idealized

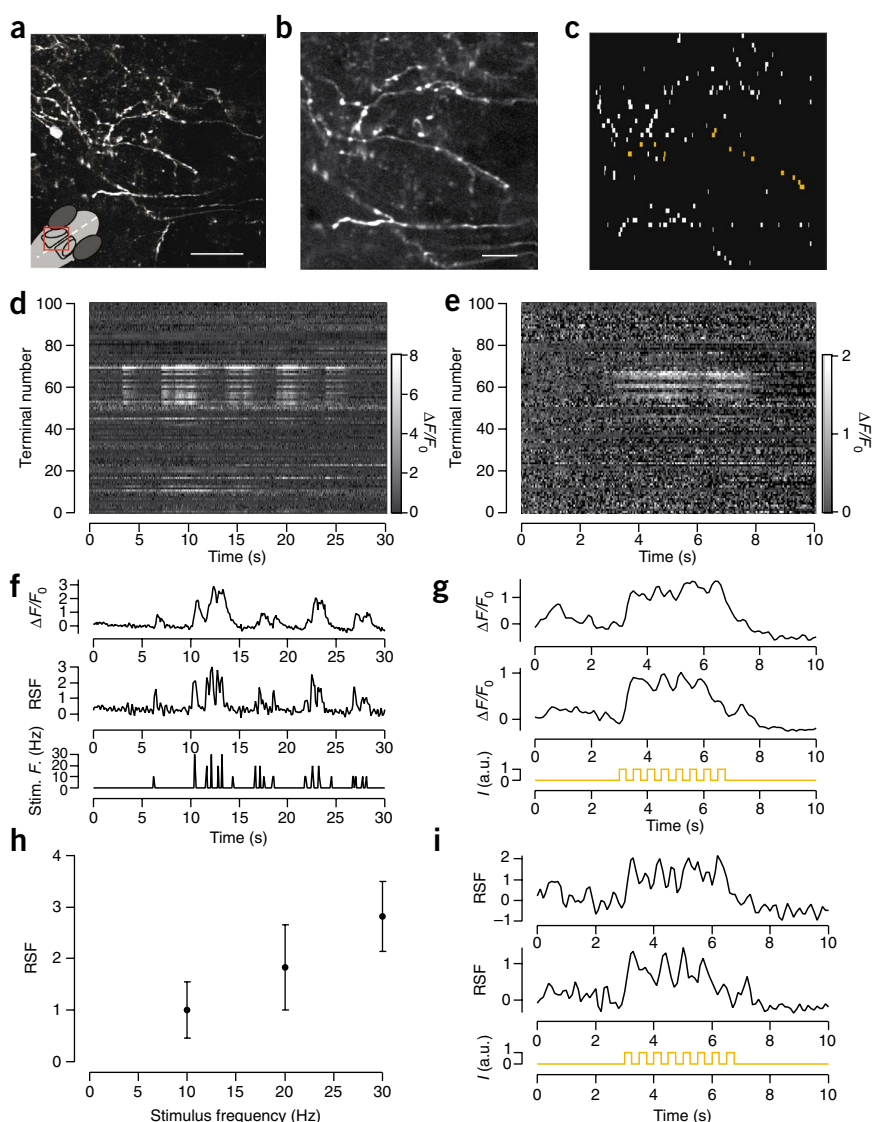


Figure 5 | Monitoring synaptic activity in the optic tectum of zebrafish. **(a)** Fluorescence image of an optic tectum of a zebrafish (9 d after fertilization) transiently expressing SyGCaMP2 under the α -tubulin promoter. The red box in the schematic (bottom left) indicates the area imaged in the head. For equipment and settings, see **Supplementary Methods**. Scale bar, 50 μ m. **(b)** Magnified fluorescence image of the optic tectum shown in **a**. Scale bar, 20 μ m. **(c)** Regions of interest corresponding to single synapses in **b**. Terminals responding to light are in amber. **(d,e)** Raster plots showing fluorescence responses from 100 terminals marked in **c**, elicited by an electric field (**d**) or a light stimulation (**e**) shown in bottom panels of **f** or **g**, respectively. Imaging frequency, 20 Hz; 256 \times 50 pixels. **(f)** SyGCaMP2 signals averaged from 12 terminals (from different areas of the tectum, same fish) (top). RSF calculated by deconvolution using the minimum impulse response (rising and decay time constants of 50 and 350 ms) (middle). Pattern of field stimulation (bottom). **(g)** Traces of two SyGCaMP2 signals from amber terminals in **c**, responding to two identical light stimuli (square wave, 100% modulation at 2 Hz, 50% duty cycle, 590 nm). The amplitude of the light responses did not exceed the average amplitude of the minimal field stimulus. **(h)** RSF plotted against the frequency of electrical stimulation (1 ms pulses) obtained from four different experiments in different areas of the tectum. Note linearity. Error bars, s.e.m. **(i)** Estimate of the RSF calculated by deconvolution of the traces in **g**.

reconstructions: single stimuli were detectable, and variations in the number of stimuli per burst were clearly observable. To summarize reconstruction accuracy, we plotted the RSF against the frequency of the minimal field stimulus (collected results from four different regions of the tectum). SyGCaMP2 signals varied linearly with stimulus frequency, validating the use of deconvolution over this range of activities.

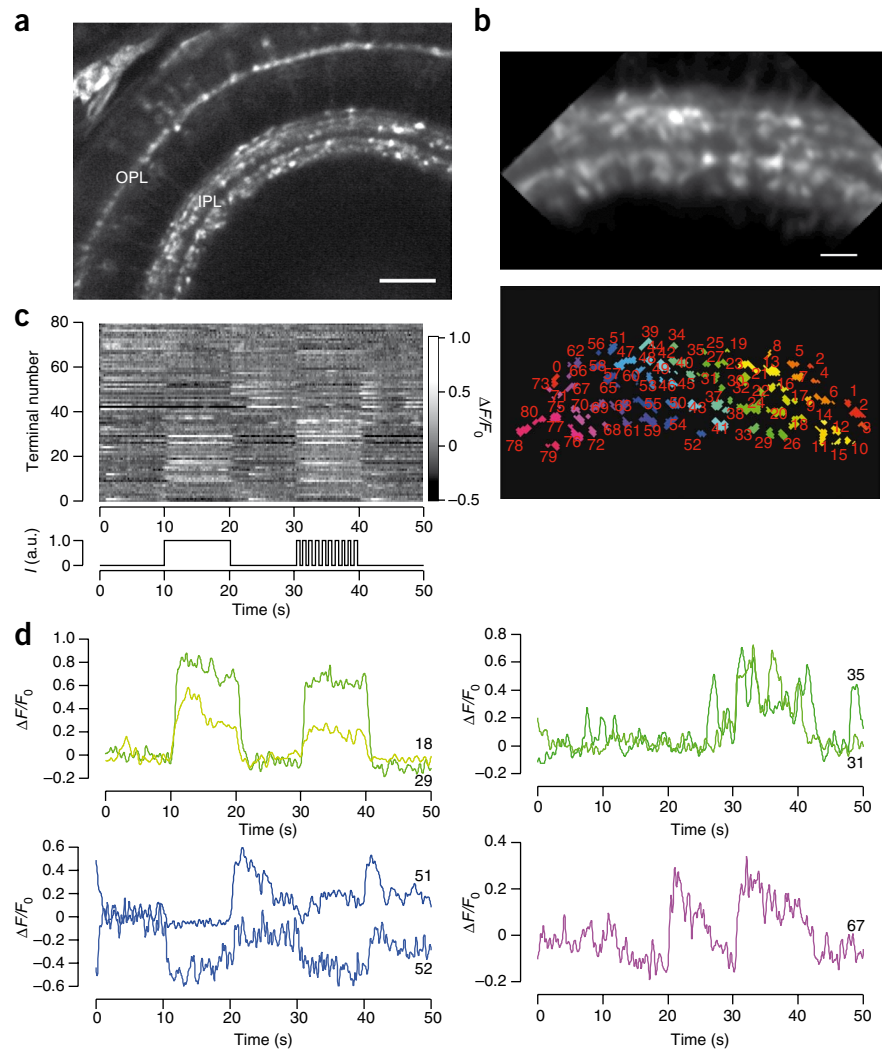
We did not use deconvolution to reconstruct the absolute spike rate from tectal neurons because this would require an electrophysiological calibration of the SyGCaMP2 signal to a single spike, which will vary from cell to cell and even synapse to synapse²⁴ (Fig. 2e,f). Further, electrophysiological calibrations of optical signals will not be practical when imaging large numbers of neurons in intact tissues. The more fundamental issue is whether the response of the reporter is linear over the range of activities of the neurons to be studied. Tectal neurons respond to light with sparse bursts of action potentials²³, implying that deconvolution of SyGCaMP2 signals will be useful for assessing electrical activity driven by a visual stimulus. We collected two examples of SyGCaMP2 responses to full-field light modulated at 2 Hz, averaged over the same population of synapses investigated by field stimulation (Fig. 5g). The peak response did not exceed 130%, falling within the linear

range assessed by field stimulation (Fig. 5f,h). Deconvolution using the kernel obtained by field stimulation yielded traces showing the relative spike frequency (Fig. 5i). Different presentation of the stimulus generated variable responses, and we often observed modulation on a subsecond timescale. These results demonstrate that SyGCaMP2 could clearly reveal synaptic activity *in vivo* and has the potential to obtain quantitative estimates of the underlying electrical activity of neurons.

Whereas synapses in the optic tectum are activated by fast action potentials and have a conventional structure, ribbon-type synapses in the retina are functionally distinct, transmitting graded voltage signals by continuously modulating the rate of vesicle release²⁵ to provide a wider repertoire of signaling. For instance, bipolar cells use ribbon synapses to transmit signals of different polarities (on or off) and kinetics (sustained or transient), establishing 'parallel channels' of information flow^{26,27}. To investigate SyGCaMP2 signals in ribbon synapses, we stably expressed the reporter in zebrafish using the *ctbp2* (also known as *ribeye a*) promoter (Fig. 6a).

In an example experiment, we monitored 80 synaptic terminals in one optical plane at intervals of 128 ms (Fig. 6b–d and **Supplementary Video 3**). We stimulated the live fish with a steady

Figure 6 | Monitoring synaptic activity in the retina of zebrafish. **(a)** The eye of a larval zebrafish (9 d after fertilization) expressing SyGCaMP2 under control of the *ribeye* promoter. Photoreceptor terminals appear in the outer plexiform layer (OPL) and bipolar cell terminals in the inner plexiform layer (IPL). Scale bar, 50 μm . **(b)** The IPL in a different fish (9 d after fertilization) expressing SyGCaMP2 (top) and the regions of interest in which SyGCaMP2 signals were measured and are numbered and shown in different colors (bottom). Scale bar, 20 μm . **(c)** Graph showing fluorescence responses from 80 terminals shown in **b**. Two light stimuli (490 nm) were applied: a steady uniform one followed by a flickering one (2-Hz square wave, 100% modulation, 50% duty cycle). Images were collected every 128 ms. **(d)** Some example traces of different types of SyGCaMP2 responses in terminals from **c**. The colors and numbers of the traces correspond to the regions of interest in **b**.



and then flickering (2 Hz) blue light. The majority of terminals showed clear modulation of the presynaptic calcium signal in response to visual stimulation (Fig. 6c). We identified several different types of responses (Fig. 6d), including sustained 'on' responses (a rise in calcium that is maintained in response to a steady light), sustained 'off' (a fall in calcium that is maintained in response to a steady light), excitatory responses to contrast but not to the steady light, and transient 'off' responses (a fast rise in calcium when the light was turned off). Thus, SyGCaMP2 allowed us to detect a fall in calcium in neurons that hyperpolarize in response to light as well as a rise in calcium when they depolarized. Such recordings could be made repeatedly over a period of hours in live fish.

DISCUSSION

The targeting of a GECI to the presynaptic terminal provides a new strategy for monitoring the electrical activation of synapses in networks of connected neurons. The sensing of the presynaptic calcium transient controlling neurotransmitter release reported the activation of a synapse with improved sensitivity and temporal resolution as compared with reporters such as synaptopHluorin^{6–8}. Assessment of the underlying electrical activity of a neuron is also possible, with improved temporal resolution and dynamic range as compared with GECIs in the soma. Detecting the time and place of signals transferred across tens to hundreds of synapses simultaneously will help us analyze the structure of neural circuits in relation to their function. GECIs localized to synaptic terminals will also help us understand how modulation of presynaptic calcium signals contributes to changes in circuit function by, for instance, activation of presynaptic receptors that regulate the activation of voltage-dependent calcium channels.

Using calcium reporters to monitor electrical activity is a tradeoff between sensitivity and dynamic range: sensitivity

requires efficient binding of calcium in response to a single spike, but this reduces the dynamic range of the reporter by saturation at higher levels of activity. For instance, GECIs that report changes in bulk calcium after a single spike saturate after as few as three¹⁴. In contrast, we found that the amplitude of SyGCaMP2 signals in small hippocampal synapses was linear with the number of APs up to about 8 at a frequency of 20 Hz, and the reporter remained far from saturation at frequencies of 20 Hz or more. This property of SyGCaMP2 may seem surprising at first, given that GCaMP2 binds Ca^{2+} ions with a cooperativity of 4 and a K_d of ~ 150 nM, but it is readily explained by the simulation in Figure 1c: the rise in presynaptic Ca^{2+} generated by an AP is very brief compared with the speed with which Ca^{2+} binds to GCaMP2, such that each bolus of Ca^{2+} only occupies a small fraction ($<2\%$) of GCaMP2 molecules. Additional support for this conclusion arises from considering the mean capture time (τ_c) of a Ca^{2+} ion entering the presynaptic terminal ($\tau_c = K_{on}^{-1} \times [\text{SyGCaMP2}]^{-1}$), which has a value of 37 ms assuming an association time constant K_{on} of 26.7 s^{-1} and a SyGCaMP2 concentration of $1 \mu\text{M}$. In comparison, a Ca^{2+} ion will take just 0.5 ms to travel $0.5 \mu\text{m}$ and escape the synaptic bouton, assuming a diffusion coefficient of $220 \mu\text{m}^2 \text{ s}^{-1}$. Thus, the great majority of Ca^{2+} ions entering during a spike successfully run the gauntlet of SyGCaMP2 molecules immobilized in the synaptic terminal,

preventing saturation with Ca^{2+} ions even when the neuron is firing at frequencies of tens of hertz. The dynamic range of synaptically localized calcium reporters might be increased further by the generation of brighter proteins with reduced affinities reflecting reduced on-rates for calcium binding.

Neurons in different regions of the nervous system show large variations in electrical activity, so calcium reporters used to monitor this activity will need different sensitivities, dynamic ranges and kinetics, according to the situation. SyGCaMP2 will be suited to monitoring activity in neurons firing at rates below ~10 Hz, as in the optic tectum of zebrafish²³. SyGCaMP2 also reports graded depolarizations and hyperpolarizations in ribbon synapses of the retina, and should be of general use in analyzing this circuit. Other factors that will determine the signals obtained using synaptically localized calcium reporters include the geometry and size of the presynaptic compartment, the density of presynaptic calcium channels and the properties of internal calcium buffers, stores and pumps. These factors vary between neurons and within neurons²⁴. Indeed, the ability of SyGCaMP2 to detect spike activity varied across different boutons of the same hippocampal neuron owing to variations in the presynaptic calcium signal. It is also notable that although the saturating response in cultured neurons was always <100% at 20 Hz, in tectal neurons *in vivo* linearity was maintained with responses up to ~300%. This difference may reflect greater calcium influx per AP in tectal neurons compared with cultured neurons.

Although SyGCaMP2 allows the locations of active synapses to be identified, it does not immediately relate this information to the morphology of individual neurons. This should become possible by combining SyGCaMP2 with cytoplasmic or membrane-targeted proteins emitting toward the blue or red parts of the spectrum, or perhaps the Brainbow approach for defining the morphology of larger numbers of interconnected neurons²⁸. We hope that the localization of a GECI to the presynaptic terminal will provide a general strategy for analyzing the functional connectivity of neural circuits by imaging.

METHODS

Methods and any associated references are available in the online version of the paper at <http://www.nature.com/naturemethods/>.

Note: Supplementary information is available on the Nature Methods website.

ACKNOWLEDGMENTS

We thank all the members of the lab for discussions, M. Jones for providing us electrophysiological data, J.-I. Nakai (RIKEN Brain Science Institute) for providing us the GCaMP2 plasmid and Martin Meyer (King's College London) for providing us the α -tubulin:Gal4/VP16 and *5UAS:EGFP-N1* plasmids. The Virtual Cell simulation environment is supported by a US National Institutes of Health grant P41RR013186 from the National Center for Research Resources. This work was supported by the Medical Research Council and the Wellcome Trust.

AUTHOR CONTRIBUTIONS

E.D. carried out molecular biology, performed and analyzed experiments, and wrote the paper; B.O. carried out molecular biology and contributed to analysis; M.M.D. wrote software and contributed to analysis; L.L. designed and performed experiments, carried out modeling and analysis, and wrote the paper.

Published online at <http://www.nature.com/naturemethods/>.

Reprints and permissions information is available online at <http://npg.nature.com/reprintsandpermissions/>.

- Garaschuk, O. *et al.* Optical monitoring of brain function *in vivo*: from neurons to networks. *Pflügers Arch.* **453**, 385–396 (2006).
- Gobel, W. & Helmchen, F. *In vivo* calcium imaging of neural network function. *Physiology (Bethesda)* **22**, 358–365 (2007).
- Pologruto, T.A., Yasuda, R. & Svoboda, K. Monitoring neural activity and $[\text{Ca}^{2+}]$ with genetically encoded Ca^{2+} indicators. *J. Neurosci.* **24**, 9572–9579 (2004).
- Reiff, D.F. *et al.* *In vivo* performance of genetically encoded indicators of neural activity in flies. *J. Neurosci.* **25**, 4766–4778 (2005).
- Mao, T., O'Connor, D.H., Scheuss, V., Nakai, J. & Svoboda, K. Characterization and subcellular targeting of GCaMP-type genetically-encoded calcium indicators. *PLoS ONE* **3**, e1796 (2008).
- Miesenböck, G., De Angelis, D.A. & Rothman, J.E. Visualizing secretion and synaptic transmission with pH-sensitive green fluorescent proteins. *Nature* **394**, 192–195 (1998).
- Ng, M. *et al.* Transmission of olfactory information between three populations of neurons in the antennal lobe of the fly. *Neuron* **36**, 463–474 (2002).
- Bozza, T., McGann, J.P., Mombaerts, P. & Wachowiak, M. *In vivo* imaging of neuronal activity by targeted expression of a genetically encoded probe in the mouse. *Neuron* **42**, 9–21 (2004).
- Katz, B. *The Release of Neural Transmitter Substances*. (Liverpool Univ. Press, Liverpool, England, 1969).
- Koester, H.J. & Sakmann, B. Calcium dynamics associated with action potentials in single nerve terminals of pyramidal cells in layer 2/3 of the young rat neocortex. *J. Physiol. (Lond.)* **529**, 625–646 (2000).
- Tallini, Y.N. *et al.* Imaging cellular signals in the heart *in vivo*: cardiac expression of the high-signal Ca^{2+} indicator GCaMP2. *Proc. Natl. Acad. Sci. USA* **103**, 4753–4758 (2006).
- Sinha, S.R., Wu, L.G. & Saggau, P. Presynaptic calcium dynamics and transmitter release evoked by single action potentials at mammalian central synapses. *Biophys. J.* **72**, 637–651 (1997).
- Granseth, B., Odermatt, B., Royle, S.J. & Lagnado, L. Clathrin-mediated endocytosis is the dominant mechanism of vesicle retrieval at hippocampal synapses. *Neuron* **51**, 773–786 (2006).
- Wallace, D.J. *et al.* Single-spike detection *in vitro* and *in vivo* with a genetic Ca^{2+} sensor. *Nat. Methods* **5**, 797–804 (2008).
- Rosenmund, C. & Stevens, C.F. Definition of the readily releasable pool of vesicles at hippocampal synapses. *Neuron* **16**, 1197–1207 (1996).
- Hanse, E. & Gustafsson, B. Vesicle release probability and pre-primed pool at glutamatergic synapses in area CA1 of the rat neonatal hippocampus. *J. Physiol. (Lond.)* **531**, 481–493 (2001).
- Yasuda, R. *et al.* Imaging calcium concentration dynamics in small neuronal compartments. *Sci. STKE* **2004**, pl5 (2004).
- Orger, M.B., Kampff, A.R., Severi, K.E., Bollmann, J.H. & Engert, F. Control of visually guided behavior by distinct populations of spinal projection neurons. *Nat. Neurosci.* **11**, 327–333 (2008).
- Yaksi, E. & Friedrich, R.W. Reconstruction of firing rate changes across neuronal populations by temporally deconvolved Ca^{2+} imaging. *Nat. Methods* **3**, 377–383 (2006).
- Hieber, V., Dai, X., Foreman, M. & Goldman, D. Induction of α -tubulin gene expression during development and regeneration of the fish central nervous system. *J. Neurobiol.* **37**, 429–440 (1998).
- Koster, R.W. & Fraser, S.E. Tracing transgene expression in living zebrafish embryos. *Dev. Biol.* **233**, 329–346 (2001).
- Gahtan, E. & Baier, H. Of lasers, mutants, and see-through brains: functional neuroanatomy in zebrafish. *J. Neurobiol.* **59**, 147–161 (2004).
- Bollmann, J.H. & Engert, F. Subcellular topography of visually driven dendritic activity in the vertebrate visual system. *Neuron* **61**, 895–905 (2009).
- Brenowitz, S.D. & Regehr, W.G. Reliability and heterogeneity of calcium signaling at single presynaptic boutons of cerebellar granule cells. *J. Neurosci.* **27**, 7888–7898 (2007).
- Odermatt, B. & Lagnado, L. Ribbon Synapses in *Encyclopedia of Neuroscience* Vol. 8 (ed. Squire, L.R.) 373–381 (Elsevier, Oxford, Academic Press, Oxford, 2009).
- Baccus, S.A. Timing and computation in inner retinal circuitry. *Annu. Rev. Physiol.* **69**, 271–290 (2007).
- Masland, R.H. The fundamental plan of the retina. *Nat. Neurosci.* **4**, 877–886 (2001).
- Livet, J. *et al.* Transgenic strategies for combinatorial expression of fluorescent proteins in the nervous system. *Nature* **450**, 56–62 (2007).

ONLINE METHODS

Molecular biology. Expression of DNA constructs in rat hippocampal neurons was obtained by transfection using Lipofectamine 2000 (Invitrogen), as described in ref. 29. To express GCaMP2 we used the vector pEGFP-N1 (Clontech) after PCR replacement of EGFP by GCaMP2 from pN1-GCaMP2 (gift from J.-I. Nakai, RIKEN) using primers GCaMP2_for and GCaMP2_rev (**Supplementary Table 2**) and BamHI and NotI restriction enzymes. Then we cloned the SyGCaMP2 construct under the control of the cytomegalovirus promoter, for expression in hippocampal cells, in two steps. First, we amplified rat synaptophysin1 cDNA (NM_012664 GI: 6981621) by PCR using ratSynp_for and ratSynp_rev primers (**Supplementary Table 2**) via XhoI and BamHI. Second, we fused GCaMP2 to the C terminus of rat synaptophysin1 in the resulting ratSynp-EGFP vector replacing EGFP by PCR amplification with SyG2_for and SyG2_rev primers (**Supplementary Table 2**) and digestion with BamHI and NotI.

To improve transgenesis of zebrafish by DNA microinjection, we designed plasmids exploiting the advantages of the I-SceI meganuclease co-injection protocol³⁰. For this purpose we cloned at both edges of the multiple cloning site of the original pBluescript II KS+ (Stratagene) an I-SceI recognition site replacing the BssHII cutting sequence by PCR amplification using I-SceI_for and I-SceI_rev primers (**Supplementary Table 2**).

To obtain the expression of SyGCaMP2 in the zebrafish retina we used a new retinal promoter for the *ribeye* protein (B.O., unpublished data), and we replaced the rat synaptophysin with the zebrafish synaptophysin. First, we ligated the *ribeye* promoter into the AleI and XbaI sites of the I-SceI pBluescript plasmid (New England Biolabs). Second, we amplified the zebrafish synaptophysin b (NM_001030242/gi:221139917) by PCR amplification using ZfSynp_for and ZfSynp_rev primers (**Supplementary Table 2**) from the cDNA IMAGE clone 7287035 and cloned into pEGFP-N1 (Clontech) digested with XhoI and BamHI. Third, we digested the zebrafish synaptophysin-EGFP fragment with NheI and SspI, and we inserted into the I-SceI pBluescript vector behind the *ribeye* promoter using SpeI and EcoRV. Finally, we replaced EGFP by GCaMP2 at the C terminus of zebrafish synaptophysin, by digestion with NotI and BamHI as described above. Expression of SyGCaMP2 under the *ribeye* promoter was stable until fish reached adulthood (6 months).

To obtain expression of SyGCaMP2 in tectal neurons we used the pan-neuronal promoter for α -tubulin with the Gal4/UAS system²¹. We performed injections using the α -tubulin:Gal4/VP16 plasmid (provided by M. Meyer as well as the 5UAS:EGFP-N1 vector) and a 5UAS:Zf-SyGCaMP2 plasmid. To obtain the 5UAS:Zf-SyGCaMP2 plasmid we started from the 5UAS:EGFP-N1 vector construct. We digested the 5UAS fragment with AseI and BglII, and we inserted this into the I-SceI pBluescript vector digested with SacI and BamHI. Then we cut the Zf-SyGCaMP2 fragment from the *ribeye*:Zf-SyGCaMP2 vector described above with AfeI, AflI, and we inserted this behind the UAS fragment of the I-SceI pBluescript vector digested with EcoRV.

Imaging synaptic activity in cultured hippocampal neurons. Primary cultures of hippocampal neurons dissociated from E18 rat pups were prepared using methods approved by the Home Office of the UK, as previously described¹³. Cells were transfected after 7 days *in vitro* using Lipofectamine 2000 in minimal

essential medium. During experiments cells were perfused with a buffer (pH 7.4) containing (in mM): 136 NaCl, 2.5 KCl, 10 HEPES (4-(2-hydroxyethyl)-1-piperazineethanesulfonic acid), 1.3 MgCl₂, 10 glucose, 2 CaCl₂, 0.01 CNQX and 0.05 DL-APV. CNQX and APV (blockers of excitatory synaptic transmission) were from Tocris Cookson and other chemicals from Sigma-Aldrich. When using ionomycin to permeabilize cells to calcium, we replaced NES buffer first with a calcium-free solution containing 10 mM EGTA and 5 μ M ionomycin (Sigma), then with 2.5 mM calcium NES buffer with 5 μ M ionomycin.

Neurons were imaged after 14 days *in vitro* using a charge-coupled device (CCD) camera (Cascade 512B; Photometrics) mounted on an inverted microscope (Nikon Diaphot 200; Kawasaki) with a 40 \times , 1.3 numerical aperture oil immersion objective. Images were captured in Frame Transfer mode at a depth of 16 bits to a Macintosh G4 computer using IPLab software (BD Biosciences). GCaMP2 was imaged with a filter set comprising 475AF40 excitation filter, a 505DRLP dichroic mirror and a 535AF45 emission filter (Omega). mRFP-VAMP was imaged using a 560AF55 excitation filter, a 595DRLP dichroic mirror and a 645AF75 emission filter. Illumination was controlled via a shutter (Uniblitz VMM-D3; Vincent Associates). In early experiments a 100-W xenon arc lamp was used for illumination and attenuated four to eight times using neutral density filters to minimize photobleaching. This lamp was found to be a high source of noise in measurements and was replaced with a light-emitting diode (LED) (Luxeon K2, blue) driven from a constant current source at 1,500 mA (**Supplementary Methods**).

APs were evoked in a custom-built chamber by field stimulation (20 mA, 1-ms pulses) across two parallel platinum wires 3 mm apart²⁹. Image sequences were obtained at 20 Hz using 45-ms integration times, then imported to Igor Pro (WaveMetrics) and analyzed using custom-written macros¹³. To measure synaptic responses, square regions of interest (ROIs) measuring $2.3 \times 2.3 \mu\text{m}$ were positioned on synapses identified by an SNR greater than 2 (ref. 13). To subtract the local background signal, the intensity of an ROI displaced in the x- or y-direction by $2.3 \mu\text{m}$ was also measured. Signals were quantified as $\Delta F/F_0$, where F_0 was measured over the 1-s period before a stimulus was applied. In all graphs, error bars are \pm s.e.m.

Generation of transgenic zebrafish. Zebrafish (*Danio rerio*) were maintained according to the national law (the Animal Act 1986) and Home Office regulations and approved by the Medical Research Council Laboratory of Molecular Biology Ethical Review Committee. We grew and kept larvae and embryos as well as adult fish as described³¹ at a 14 h–10 h light-dark cycle at 28 °C and bred naturally. To generate a transgenic line *tg(ribeye:Zf-SyGCaMP2)* we followed a published protocol³¹ using wild-type zebrafish with a mixed genetic background, originally purchased from a local pet shop, and fish homozygous for the *roy orbison* (*roy*) mutation³². The *roy* mutants are characterized by reduced numbers of iridophores, which allow high-resolution imaging at later ages (up to 2 weeks after fertilization). Studies on *roy* mutants do not report abnormalities of the IPL or impaired visual performance tasks.

For the transient expression of the SyGCaMP2 indicator in tectal neurons, we co-injected α -tubulin:Gal4/VP16 plasmid and the UAS:Zf-SyGCaMP2 plasmid with I-SceI meganuclease into the one-cell stage fertilized following guidelines in ref. 30.



For fish expressing fluorescent proteins we always added PTU (1-phenyl-2-thiourea, 200 μ M final concentration; Sigma) to the E2 fish medium from 28 hours postfertilization (hpf) on to inhibit melanin formation³³. To assess fluorescence expression in the retina we screened embryos using an epifluorescence stereomicroscope (Olympus X12) between 36 and 48 hpf. In this manner we obtained one transgenic zebrafish line expressing SyGCaMP2 *tg(ribeye:Zf-SyGCaMP2)*.

Imaging synaptic activity in the retina of zebrafish. Larval zebrafish (9–10 d after fertilization) were anesthetized by immersion in 0.016% MS222 (Sigma) and immobilized in 2.5% low-melting agarose (Biogene) on a glass slide. For imaging the retina through the pupil, fish were mounted with one eye pointing toward the objective. For imaging the tectum through the skin, they were placed belly down facing forward. Ocular muscles were paralyzed by injection of α -bungarotoxin (2 mg ml⁻¹) next to the eye. Imaging was carried out using a custom-built two-photon microscope³⁴ equipped with a mode-locked Chameleon titanium-sapphire laser tuned to 915 nm (Coherent). The objective was an Olympus LUMPlanFI 40 \times water immersion (NA 0.8). The intensities of exciting illumination bleached SyGCaMP2 at rates of \sim 9% per minute. Emitted fluorescence was captured by the objective and by a substage condenser, and in both cases filtered by an HQ 535/50GFP emission filter (Chroma Technology) before detection by photomultiplier tubes (Hamamatsu). Scanning and image

acquisition were controlled using ScanImage v. 3.0 software³ running on a PC. Light stimuli were delivered by a blue or amber LED projected through the objective onto the retina. Electric field stimulation was delivered mounting the fish in the same custom-built chamber used for the hippocampal cells. Timing of stimulation was controlled through Igor Pro v. 4.01 software running on a Macintosh, which also triggered image acquisition. Image sequences were acquired at 1 ms per line using 256 \times 50 or 128 \times 128 pixels per frame and analyzed with custom-written macros in Igor Pro v. 6.10 or ImageJ v. 1.39 (NIH). ROIs corresponding to synaptic terminals were defined by transforming images using a Laplace operator followed by thresholding (**Supplementary Methods**).

29. Royle, S.J., Granseth, B., Odermatt, B., Drevier, A. & Lagnado, L. Imaging phluorin-based probes at hippocampal synapses. *Methods Mol. Biol.* **457**, 293–303 (2008).
30. Thermes, V. *et al.* I-SceI meganuclease mediates highly efficient transgenesis in fish. *Mech. Dev.* **118**, 91–98 (2002).
31. Nusslein-Volhard, C. & Dahm, R. *Zebrafish*, 1st ed. (Oxford University Press, Oxford, New York, 2002).
32. Ren, J.Q., McCarthy, W.R., Zhang, H., Adolph, A.R. & Li, L. Behavioral visual responses of wild-type and hypopigmented zebrafish. *Vision Res.* **42**, 293–299 (2002).
33. Karlsson, J., von Hofsten, J. & Olsson, P.E. Generating transparent zebrafish: a refined method to improve detection of gene expression during embryonic development. *Mar. Biotechnol. (NY)* **3**, 522–527 (2001).
34. Tsai, P.S. *et al.* in *In Vivo Optical Imaging of Brain Function* (ed. Frostig, R.D.) 113–171 (CRC Press, New York, 2002).